Electronic supplementary information (ESI)

Turning Waste into Wealth: Efficient and Rapid Capture of Gold from Electronic Waste with Thiourea Functionalized Magnetic Core Stirring Rods Adsorbent and Their Application for Heterogeneous Catalysis

Hao Li,*[a,b,c] Yang Pan,[a] Fan Wu,[a] Yingying Zhou,[a] Jianming Pan*[a]

a School of Chemistry and Chemical Engineering, Jiangsu University, Zhenjiang 212013, Jiangsu, China. E-mail: haoli5385@ujs.edu.cn; pjm@ujs.edu.cn

b Anhui Laboratory of Molecules-Based Materials, College of Chemistry and Materials Sciences, Anhui Normal University, Wuhu 241002, Anhui, China.

c Jiangsu Provincial Key Laboratory of Environmental Science and Engineering, Suzhou University of Science and Technology, Suzhou 215009, Jiangsu, China.

1. Preparation of monodisperse Fe_3O_4 nanoparticles (Fe_3O_4 NPs)[1]

In a nutshell, $FeCl_3$ $6H_2O$ (3.2 g) was added to ethylene glycol (100 mL), then $Na_3Cit{\cdot}2H_2O$ (1.2 g), NaAc (5.6 g) were successively added, and mixed evenly and treated with ultrasound for 1 h, until the orange transparent solution was formed. The mixture was transferred to a hydrothermal reaction kettle and reacted at 200 ℃ for 10 h, after naturally cooling to room temperature, separated by centrifugation and washed with deionized water and ethanol for several times to remove the residual reagent. The resulting solid were dried overnight in a vacuum oven at 35 ℃ for later use.

2. Preparation of magnetic core stirring rods (MCSR)[2]

MCSR were prepared were synthesized via hydrolytic condensation of silica precursor and magnetic field induced assembly in previous reports. In a typical process, Fe_3O_4 NPs above (50 mg) was placed in a 100 mL three-necked flask, and then 60 mL ethanol was added. After ultrasonic dispersion for 5 min, it was placed in a water bath at 30 °C, added $NH_3{\cdot}H_2O$ (3.4 mL) and mechanically stirred for 20 min at 700 rpm, then reduced to 300 rpm, TEOS (0.3 mL) was added and continuous stirring for 15 min. Finally, it was placed directly above the bar magnet with a central magnetic field intensity of about 7.6 mT and stopped for 100 s, and then slowly placed in a stable place for 12 h. MCSR were separated by magnets and rinsed several times with high purity deionized water and ethanol, then dried in vacuum at 35 ℃ overnight for future use.

3. Preparation of vinyl functionalized magnetic core stirring rods (MCSR-MPS)

100 mg MCSR prepared in the above steps were dispersed in 40 mL ethanol and 10 mL deionized water. After ultrasonic dispersion for 5 min, $NH_3{\cdot}H_2O$ (1.5 mL) and MPS (0.2 mL) were successively added at 70 ℃ and 800 rpm, and stirred continuously for 24 h. The products were separated by magnets, washed several times with deionized water and ethanol, and it was dried for later use.

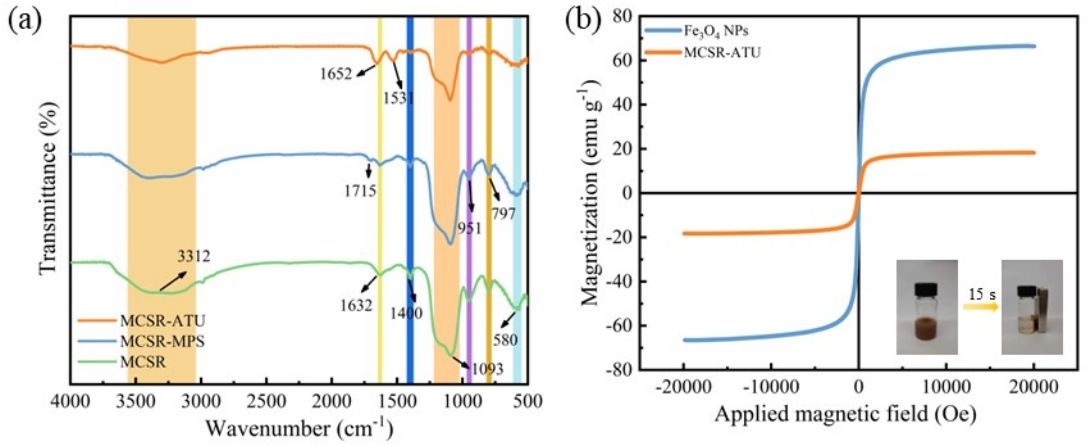

Fig. S1 (a) FT-IR spectra of adsorbent in different modification steps. (b) The VSM of Fe_3O_4 NPs and MCSR-ATU.

4. The details of the adsorption experiments

In order to determine the optimal conditions for capture gold ions by MCSR-ATU, the adsorption experiment was carried out by adding MCSR-ATU (4 mg) to a 10 mL screw-top glass bottle containing 4 mL of the adsorption solution, and then put it onto a magnetic stirrer to stir at a rate of 1000 rpm for the desired time. The prepared Au(III) stock solution was diluted to the desired concentration, during which the pH value of the solution was adjusted with NaOH (0.1 M) and HCl (0.1 M) solutions. The mixed suspension was separated by a magnet, and then the concentration of the metal ion was measured using ICP-OES. The equilibrium adsorption capacity (Q_e, mg g^{-1}) and adsorption efficiency (R %) were calculated by Eq. (1), and Eq. (2), respectively.

$$Q_e = \frac{C_0 - C_e}{M} \times V \qquad (1)$$

$$R\ \% = \frac{C_0 - C_e}{C_0} \times 100 \qquad (2)$$

Where C_0 (mg L^{-1}) and C_e (mg L^{-1}) are the original and equilibrium concentrations of Au(III), respectively. V (L) refers to the volume of solution (L). M (g) expresses the mass of the adsorbent.

Table S1 Elemental analysis results and adsorption properties of adsorbents obtained by distilling different volumes of acetonitrile.

Distilled acetonitrile (mL)	Element content (%)[a]			Monomer loading (mmol g^{-1})[b]	Q_e[c] (mg g^{-1})
	N	C	H		
5	1.89	9.79	1.95	0.675	53.58
10	2.75	10.70	2.10	0.982	78.78
15	3.44	12.69	2.35	1.229	117.95
20	4.35	15.40	2.68	1.554	139.02
25	5.97	19.20	3.22	2.068	146.89
30	4.05	14.20	2.53	1.446	122.62

[a] Determined by an elemental analyzer (EA, Flash 1112A, USA); [b] Calculated from the N elemental analysis. [c] Represents the maximum adsorption capacity.

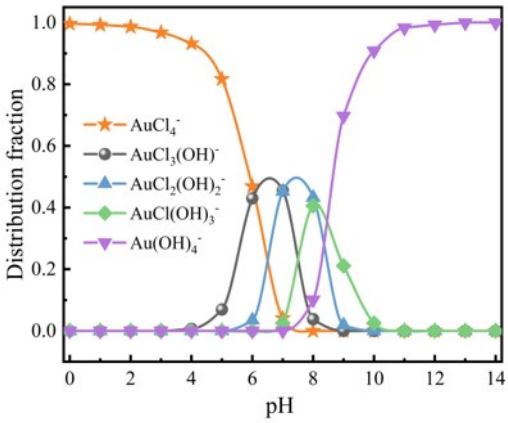

Fig. S2 The species distribution of gold ions at different pH.

5. The details of the adsorption kinetic experiments

All tested solutions had an initial concentration of 50 mg L^{-1} and the pH was fixed at 1.0 for kinetic experiments. The adsorption time ranged from 1 to 60 min.

The following lists the equations of pseudo-first-order (3), pseudo-second-order (4), intra-particle diffusion (5).[3,4]

$$Q_t = Q_e(1 - e^{-K_1 t}) \quad (3)$$

$$Q_t = \frac{K_2 Q_e^2 t}{1 + K_2 Q_e t} \quad (4)$$

$$Q_t = K_{id} t^{0.5} + C_{id} \quad (5)$$

Q_e (mg g^{-1}) stands for the amount of Gold(III) adsorbed at equilibrium, Q_t (mg g^{-1}) is adsorption capacity at time t, K_1 (min^{-1}), K_2 (g mg^{-1} min^{-1}) and K_{id} (g mg^{-1} $min^{-1/2}$) are adsorption rate constant respectively. C_{id} represents the characteristic constant of the boundary layer.

Table S2 Adsorption kinetic parameters at different stirring rates.

Stirring rate (rpm)	**Pseudo-first-order**			**Pseudo-second-order**		
	K_1 (min^{-1})	Q_e (mg g^{-1})	R^2	K_2 (g mg^{-1} min^{-1})	Q_e (mg g^{-1})	R^2
0	0.190	118.79	0.825	0.00350	123.74	0.980
100	0.209	128.36	0.807	0.00381	133.08	0.991
500	0.221	134.14	0.796	0.00399	138.71	0.988
1000	0.235	147.21	0.784	0.00406	148.29	0.986
Intra-particle diffusion model (at 1000 rpm)						
K_{id1}	K_{id2}	R_{id1}	R_{id2}	C_{id1}	C_{id2}	
8.237	0.263	0.993	0.968	102.67	147.11	

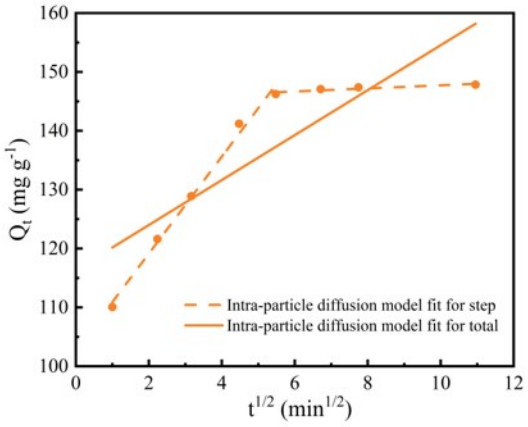

Fig. S3 The intra-particle diffusion model fit curves.

6. The details of the isothermal adsorption experiments

In the adsorption equilibrium experiment, Langmuir, Freundlich, Temkin, Hill, Redlich-Peterson (R-P) and Dubinin-Radushkevich (D-R) isotherm models were used

to analyze the equilibrium data, which can be calculated through following equations, respectively.[5-8]

$$Q_e = \frac{Q_m k_L C_e}{1 + k_L C_e} \quad (6)$$

$$Q_e = K_F C_e^{1/n} \quad (7)$$

$$Q_e = \frac{RT}{b} \ln K_T C_e \quad (8)$$

$$Q_e = \frac{Q_m C_e^n}{K_H + C_e^n} \quad (9)$$

$$Q_e = \frac{K_{R-P} C_e}{1 + A C_e^b} \quad (10)$$

$$Q_e = Q_m \exp(-K_{D-R}\varepsilon^2) \quad (11)$$

$$E = \frac{1}{\sqrt{2K_{DR}}} \quad (12)$$

where K_L (L g^{-1}), K_F ((mg g^{-1}) (mg $L^{-1})^{-(1/n)}$), K_T (L g^{-1}), K_H (mL g^{-1}), K_{R-P} (L g^{-1}) and K_{D-R} (mol^2 kJ^{-2}) are the constants of the models, Q_m (mg g^{-1}) is the maximum adsorption capacities, n, b (J mol^{-1}) and A (L mg^{-1}) are constants of the models, E (kJ mol^{-1}) is the average adsorption energy, ε is polanyi potential and $\varepsilon = RT\ln(1+1/C_e)$, T is the absolute temperature (in Kelvin).

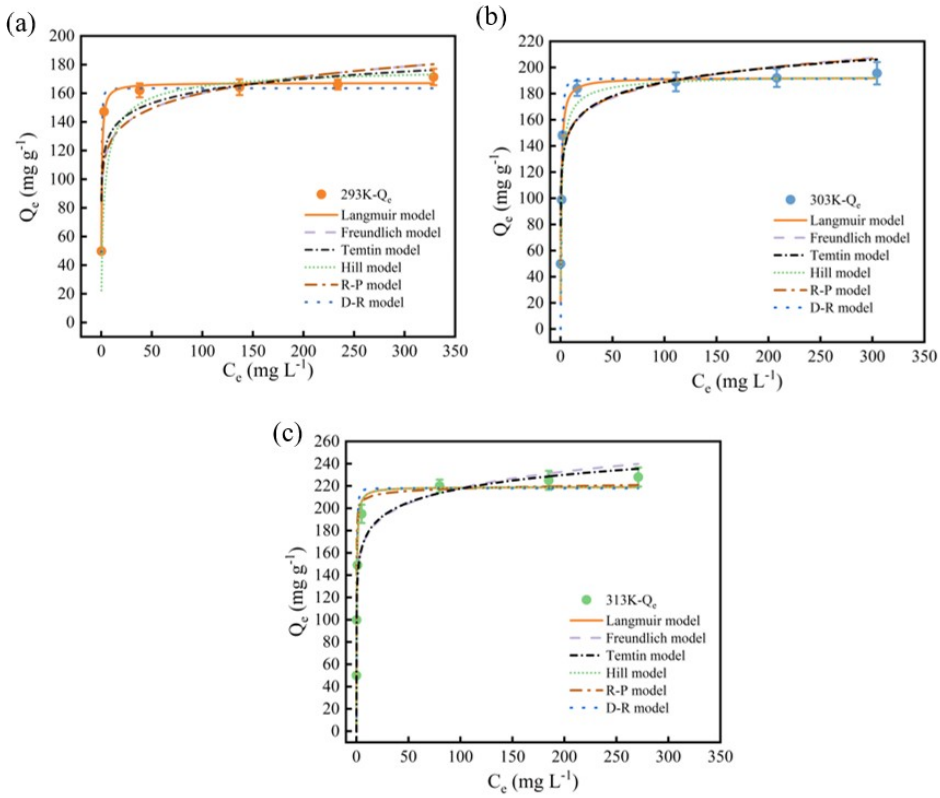

Fig. S4 The adsorption isotherm model fit curves of Au(III) on MCSR-ATU (a) 293 K (b) 303K (c) 313 K.

Table S3 The fitting parameters for the adsorption of Au(III) on MCSR-ATU using several isotherm models.

Model	**parameters**	**T (K)**		
		293	303	313
Langmuir	Q_m (mg g^{-1})	169.27	192.18	219.32
	K_L (L g^{-1})	1.252	1.420	3.120
	R^2	0.995	0.996	0.984
Freundlich	K_F ((mg g^{-1}) (mg L^{-1})$^{-(1/n)}$)	112.86	124.92	132.04
	1/n	0.0727	0.0888	0.0943
	R^2	0.968	0.925	0.941
Redlich-Peterson (R-P)	A(L mg^{-1})	1.436	8.279	12.288
	b (J mol^{-1})	0.947	0.917	0.986
	K_{R-P} (L g^{-1})	180.65	1067.9	2514.9
	R^2	0.931	0.984	0.874

Dbinin-Radushkevich (D-R)	Q_m (mg g^{-1})	164.45	189.46	217.97
	K_{D-R} (mol^2 kJ^{-2})	8.04E-6	4.76E-7	6.05E-8
	R^2	0.968	0.977	0.957
	E (kJ mol^{-1})	249.38	1024.90	2874.79
Temkin	b (J mol^{-1})	197.95	162.95	145.32
	K_T (L g^{-1})	3740.2	2016.1	1886.4
	R^2	0.981	0.993	0.938
Hill	Q_m (mg g^{-1})	170.29	195.01	219.15
	K_H (L mg^{-1})	1.400	1.025	0.321
	n	0.701	0.742	0.998
	R^2	0.974	0.977	0.943

7. The details of thermodynamic parameters for adsorption Au(III) onto MCSR-ATU

Three basic thermodynamic parameters,enthalpy change (ΔH), entropy change (ΔS) and Gibbs free energy change (ΔG) were calculated by using the following equations:[7-10]

$$K = \frac{Q_e}{C_e} \quad (13)$$

$$\triangle G = -RT\ln K \quad (14)$$

$$\ln K = \frac{\Delta S}{R} - \frac{\Delta H}{RT} \quad (15)$$

where K is the adsorption equilibrium constant, $\triangle$G represents Gibb's free energy change, $\triangle$H is enthalpy change and entropy change is $\triangle$S, R is the gas constant (8.314 J mol^{-1} K^{-1}).

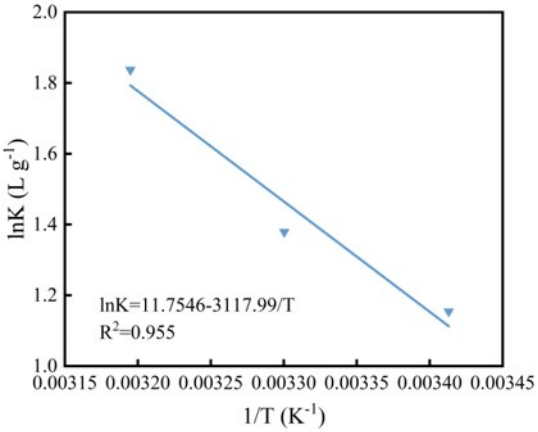

Fig. S5 The plots of lnK versus 1/T at C_0 =200 mg L^{-1}.

Table S4 Related parameters of the thermodynamic experiment.

T (K)	lnK	△G (kJ mol^{-1})	△H (kJ mol^{-1})	△S (J $mol^{-1}·K^{-1}$)
293	1.154	-2.812		
303	1.379	-3.474	25.923	97.728
313	1.837	-4.780		

8. The details of the selective adsorption experiments

The selective performance of MCSR-ATU was evaluated by the distribution coefficient (K_d), the selective coefficient (α) and the concentration coefficient (CF) using Eq. (14), Eq. (15) and Eq. (16) as follows.

$$K_d = \frac{C_0 - C_e}{C_e} \times \frac{V}{M} \quad (16)$$

$$\alpha = \frac{K_{d(Au)}}{K_{d(\text{coexisting ions})}} \quad (17)$$

$$CF = \frac{Q_e}{C_0} \quad (18)$$

Table S5 The parameters of selective adsorption.

Metal ions	C_0 (mg L^{-1})	Q_e (mg g^{-1})	K_d (L g^{-1})	CF (mL g^{-1})	α (× 10^3)
Au(III)	50.00	49.88	405.50	997.54	
Al(III)	52.21	0.26	0.0053	5.27	76.58
Co(II)	49.15	0.13	0.0027	2.66	151.72
Cr(III)	45.48	2.09	0.046	44.37	8.73
Cu(II)	48.21	0.62	0.013	12.78	31.33
Mn(II)	48.11	0.031	0.00062	0.62	649.91
Na(I)	48.2	0.011	0.00021	0.21	1954.21
Ni(II)	44.66	0.39	0.0089	8.80	45.67
Zn(II)	46.62	0.15	0.0031	3.11	130.09

Table S6 Main element content of PCB used in this work.

Element	C_0 (mg L^{-1})	C_e (mg L^{-1})			Average of C_e	Capture rate (%)
Au	3.4925	0.2121	0.1718	0.1756	0.1865	94.66
Na	1037.6	1039.7	1042.7	1045.7	1042.7	-0.492
Mg	1.2522	1.2821	1.2522	1.2268	1.2537	-0.112
Al	1.6052	1.5691	1.6052	1.6626	1.6123	-0.442
K	248.07	244.25	244.41	244.54	244.40	1.479
Ca	6.5373	6.5055	6.5527	6.5999	6.5527	-0.235
Ti	0.0579	0.0581	0.0578	0.0575	0.0578	0.176
Cr	0.6355	0.6344	0.6412	0.6264	0.6340	0.236

Mn	0.3557	0.3495	0.3565	0.3635	0.3565	-0.225
Fe	58.636	58.634	59.224	58.044	58.634	0.003
Co	6.1815	6.0779	6.2146	5.9427	6.0784	1.668
Ni	153.94	151.44	154.69	148.19	151.44	1.624
Cu	77.215	68.346	69.157	69.965	69.156	10.43
Zn	24.054	23.819	24.376	24.936	24.377	-1.343
Rb	0.0124	0.0127	0.0120	0.0122	0.0123	0.079
Sr	0.5932	0.5751	0.5842	0.5933	0.5842	1.518
Y	0.0123	0.0124	0.0124	0.0121	0.0123	-0.454
Pd	0.0526	0.0501	0.0488	0.0491	0.0493	6.212
Ag	0.0302	0.0248	0.0236	0.0248	0.0244	19.28
Te	0.0168	0.0174	0.0187	0.0185	0.0182	-8.333
Gd	0.0252	0.0256	0.0252	0.0257	0.0255	-1.191
Ho	0.0195	0.0197	0.0186	0.0190	0.0191	1.926
W	0.2607	0.2578	0.2608	0.2641	0.2609	-0.057
Pb	1.0907	1.0927	1.1177	1.1127	1.1077	-1.559
Bi	0.1579	0.1455	0.1413	0.1516	0.1468	7.006
Li	0.0292	0.0286	0.0295	0.0286	0.0289	1.027

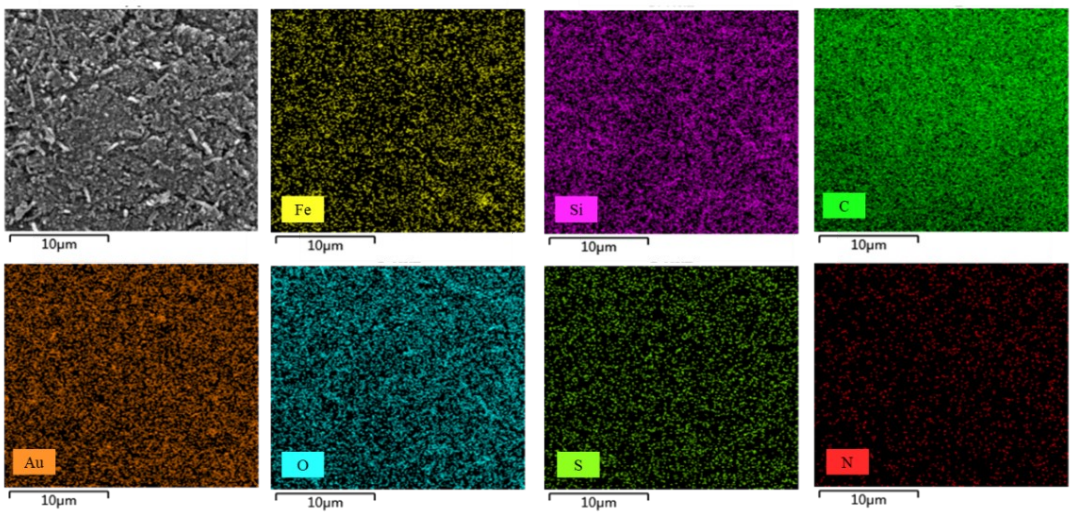

Fig. S6 The SEM-mapping images of MCSR-ATU-Au

9. The catalytic application of MCSR-ATU-Au

The reaction time t shows a good linear correlation with $\ln(C_t/C_0)$, and the reaction rate constant (k) was calculated using Eq. (19).

$$\ln (C_t/C_0) = kt + C \qquad (19)$$

where C_t and C_0 indicate the absorbance of 4-NP at t and 0 min, respectively, C is a constant.

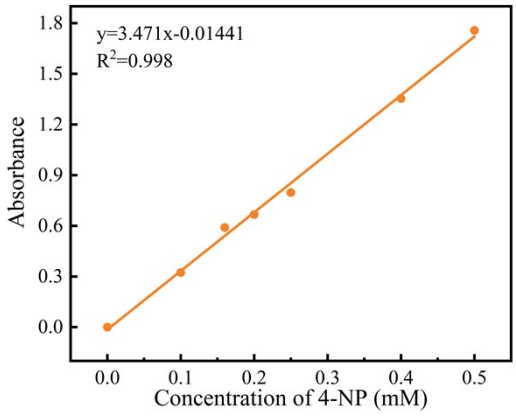

Fig. S7 A calibration curve of 4-NP

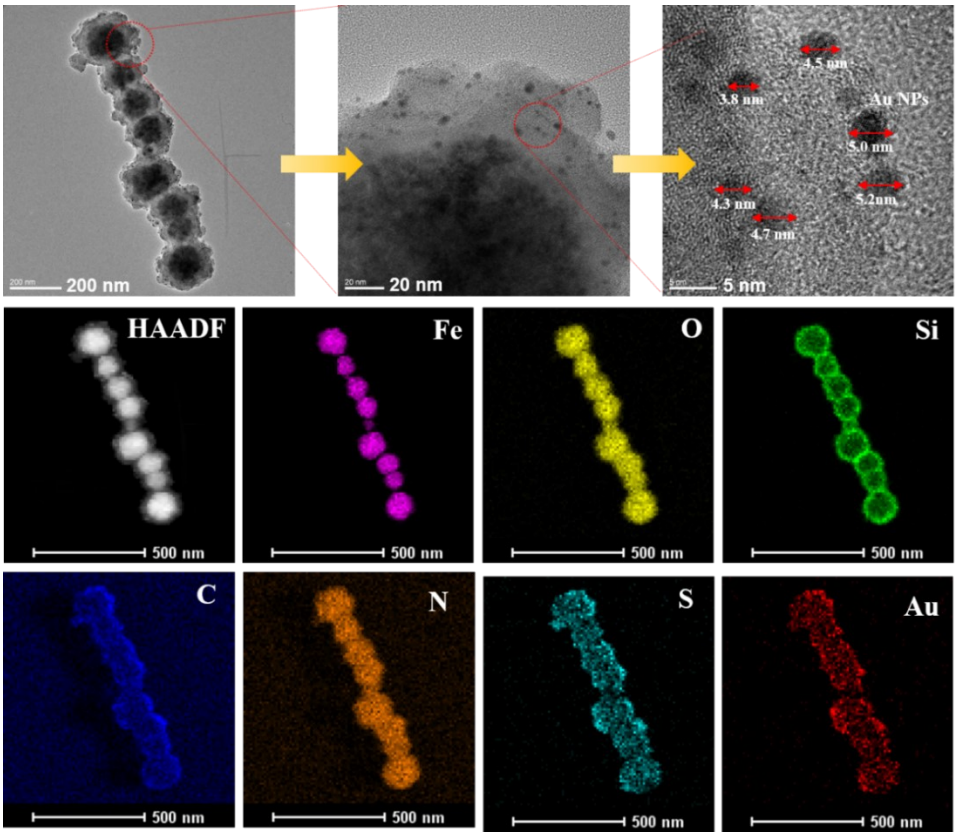

Fig. S8 The HRTEM images of the recovered MCSR-ATU-Au

References

1 J. Liu, Z. Sun, Y. Deng, Y. Zou, C. Li, X. Guo, L. Xiong, Y. Gao, F. Li and D. Zhao, *Angew. Chem., Int. Ed.*, 2009, **48**, 5875-5879.

2 L. Wan, H. Song, X. Chen, Y. Zhang, Q. Yue, P. Pan, J. Su, A. A. Elzatahry and Y. Deng, *Adv. Mater.*, 2018, **30**, e1707515.

3 Z. He, L. He, J. Yang and Q. Lü, *Ind. Eng. Chem. Res.*, 2013, **52**, 4103-4108.

4 M. Zhang, Z. Dong, F. Hao, K. Xie, W. Qi, M. Zhai and L. Zhao, *Sep. Purif. Technol.*, 2021, **274**, 119016.

5 Y. Geng, J. Li, W. Lu, N. Wang, Z. Xiang and Y. Yang, *Chem. Eng. J.*, 2020, **381**, 122627.

6 Y. Song, S. Chen, N. You, H. Fan and L. Sun, *Chemosphere*, 2020, **255**, 126917.

7 J. Guo, X. Fan, J. Wang, S. Yu, M. Laipan, X. Ren, C. Zhang, L. Zhang and Y. Li, *Chem. Eng. J.*, 2021, **425**, 130588.

8 G. Yang, Y. Liu, H. Li, X. Tian and J. Pan, *Sep. Purif. Technol.*, 2021, **266**, 118540.

9 F. Gimbert, N. M. Crini, F. Renault, P. M. Badot and G. Crini, *J. Hazard. Mater.*, 2008, **157**, 34-46.

10 Y. Liu, *J. Chem. Eng. Data*, 2009, **54**, 1981–1985.